Misfit-Induced Modification of Structure and Magnetism in O/Fe(001)-$p(1 \times 1)$

W. Feng,[1] H. L. Meyerheim,[1,*] K. Mohseni,[1] O. Brovko,[1] V. S. Stepanyuk,[1] N. Jedrecy,[2] R. Felici,[3] and J. Kirschner[1,4]

[1]*Max-Planck-Institut für Mikrostrukturphysik, Weinberg 2, D-06120 Halle, Germany*

[2]*Institut des Nano Sciences de Paris, UPMC-Sorbonne Universités, CNRS-UMR7588, 75005 Paris, France*

[3]*ESRF, B.P. 220, F-38043 Grenoble Cedex, France*

[4]*Institut für Physik, Martin-Luther-Universität Halle-Wittenberg, D-06099 Halle, Germany*

(Received 17 January 2013; revised manuscript received 8 March 2013; published 6 June 2013)

The geometry of oxygen atoms in hollow sites of Fe nanoislands ($\oslash \approx 1$–2 nm) on Fe(001) is modified by mesoscopic misfit-induced relaxations of the island atoms. Surface x-ray diffraction, scanning tunneling microscopy, and *ab initio* calculations indicate a 0.3 Å increased adsorption height [0.7 Å versus 0.4 Å in O/Fe(001)-$p(1 \times 1)$] of O atoms going in parallel with a reduced Fe-Fe layer spacing inducing a reduction of the surface magnetic moment ($2.85\mu_B$ versus $3.2\mu_B$). Our results demonstrate the importance of the mesoscopic misfit for surface physical properties in general.

DOI: 10.1103/PhysRevLett.110.235503 PACS numbers: 61.05.cp, 68.37.Ef, 68.43.Bc, 68.43.Fg

The fascinating properties of nanoscale materials stem from their unique structural property, namely, the presence of a large fraction of low coordinated atoms. In 1947, Pauling suggested that a reduced number of bonds should result in a shorter interatomic distance [1]. Also, the Smoluchowski smoothing of the charge density induces an inward contraction of surface and rim atoms [2]. Although these views were established more than half a century ago, only a few quantitative studies have been published, providing evidence for the finite size driven rearrangement of atoms in two- (2D) and three-dimensional nanoscale systems [3–5].

In this context, simple hetero- or homoepitaxial systems like Co/Cu(001) or Fe/Fe(001) where the adatoms form 2D nanoislands of $\approx$1–2 nm in diameter represent prototype systems. For instance, in the case of Co/Cu(001), molecular dynamics calculations by Stepanyuk *et al.* [6] have predicted a reduction of the average interatomic distance by up to 5% (≈ 0.10 Å) relative to the bulk value (2.51 Å). Results of experimental studies on Co nanoislands grown in monoatomic height on Cu(001) [4,5] were in perfect agreement with these predictions. The atomic rearrangement, which is commonly referred to as "mesoscopic misfit" (MM) has wide implications on the physical properties of nanoscale adsorbate systems also. For instance, using scanning tunneling spectroscopy experiments on Co/Cu(111), Rastei *et al.* [7] found island size-dependent changes of the energetic positions of the occupied and unoccupied surface states.

Nevertheless, understanding the MM-induced rearrangement of the surface atomic structure and its consequences for surface physical properties is just at the beginning. For our investigations of the MM-induced changes of the atomic geometry, we have chosen the homoepitaxial interface structure Fe/O/Fe(001)-$p(1 \times 1)$, since almost perfect layer-by-layer growth is achieved owing to the surfactant effect of oxygen atoms adsorbed on the Fe(001) surface prior to deposition of Fe [8]. Also, the O/Fe(001)-$p(1 \times 1)$ surface has been thoroughly investigated with regard to its structure and magnetic properties [9–17]. Oxygen is located in the fourfold hollow sites of the Fe(001) surface at a vertical height of 0.48 ± 0.08 Å. The concomitant expansion of the first Fe-Fe interlayer distance to 1.66 ± 0.02 Å [16] is related to an increase of the surface magnetic moment as predicted theoretically [10] and verified experimentally using second harmonic generation (SHG) [14] and spin polarized metastable deexcitation spectroscopy (SPMDS) [11]. Both studies indicated an oscillatory behavior of the surface magnetic moment with maxima and minima at full and half-filled layers, respectively. Although it is tempting to speculate that there is a direct relation between the surface magnetic moment with the surface structure, no quantitative analysis providing atomically resolved data exists so far.

We have carried out surface x-ray diffraction (SXRD) and scanning tunneling microscopy (STM) experiments combined with *ab initio* calculations to elucidate the atomic geometry of submonolayer (ML) thick Fe films grown on O/Fe(001)-$p(1 \times 1)$. We find quantitative evidence for MM-driven modifications of the adsorption geometry involving changes of the oxygen adsorption position and of the Fe-Fe interlayer spacing, the latter sensitively influencing the surface magnetic properties [10,13]. Our results provide evidence for the importance of the MM concept which goes far beyond the simple epitaxial systems studied so far.

Experiments were carried out in an ultra-high-vacuum system equipped with a variable temperature STM and at the beam line ID03 of the European Synchrotron Radiation Facility in Grenoble, France. The Fe(001) crystal was prepared following the procedure described by Kirschner [18] to achieve a surface free of contaminants within the sensitivity limit of Auger-electron spectroscopy. The

O/Fe(001)-$p(1 \times 1)$ surface was prepared by dosing about 10 L of oxygen at a pressure of 1×10^{-8} mbar followed by annealing at 500 °C for 1 min. Subsequently, Fe was deposited on the sample kept at room temperature by evaporation from an Fe rod heated by electron bombardment.

Formation of a well-ordered O/Fe(001)-$p(1 \times 1)$ surface was verified by SXRD (see below). The intensity distribution along the crystal truncation rods (CTRs) were in perfect agreement with corresponding data collected earlier [16]. A 2D pixel detector allows for the precise collection of diffraction intensities by at least 2 orders of magnitude faster than previously possible by using a point detector [19]. The amount of Fe deposited was calibrated by the intensity oscillations at the antiphase (01 0.1) scattering condition. First, we discuss the STM experiments.

Figure 1 shows an 8.0×3.6 nm^2 constant current STM image of two Fe islands ($U = -0.2$ V, $I = 100$ pA) of about 4 nm (left) and 1.5 nm (right) in diameter. In this experiment, 0.18 ML Fe were deposited (here, and in the following, 1 ML corresponds to one adatom per substrate atom, i.e., 1.20×10^{15} atoms/cm^2). This sample was prepared by mild annealing (150 °C) to achieve an inhomogeneous size distribution.

The O/Fe(001)-$p(1 \times 1)$ structure on the substrate surface and in the center of the large island is atomically resolved, where the protrusions are related to the adsorbed oxygen atoms [17]. Note that a distinct difference with regard to geometric and/or electronic structure exists between the flat O/Fe(001)-$p(1 \times 1)$ structure and that at the rim of the large nanoisland, which is related to the increased STM contrast and the lack of atomic resolution. If the island diameter becomes smaller than 2–3 nm, the island is characterized by the ''rim state'' as can be seen for the small island.

The inset shows the profile along the white line starting from the lower terrace running across the small and the large island. We find a (apparent) height difference of approximately 2 Å between the lower terrace and the island rims and a height difference of 0.75 Å between the island rim and the island center. There is also a height difference of ≈2 Å between the levels of the terrace and the small island, indicating a close resemblance between their structures.

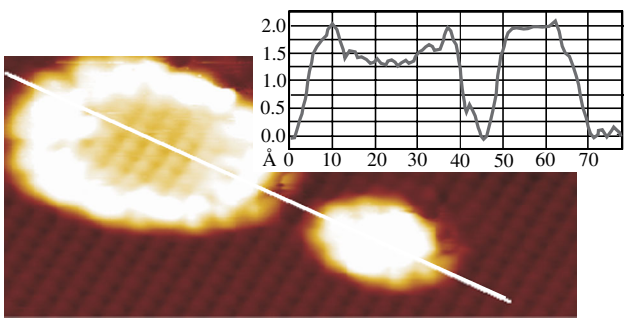

FIG. 1 (color online). Constant current ($U = -0.2$ V sample bias, $I = 100$ pA) STM image (8×3.6 nm^2) showing two differently sized Fe nanoislands deposited on O/Fe(001)-$p(1 \times 1)$. The profile along the line is shown in the inset.

In a second step, SXRD experiments were carried out to derive quantitative structure parameters. In total, seven data sets were collected after depositing Fe between 0.25 and 1.50 ML, each after the preparation of a fresh surface. In general, for each data set, about 600 reflections were collected reducing to approximately 300 by symmetry equivalence after averaging on the basis of the $p4mm$ plane group symmetry. The reproducibility of symmetry equivalent reflections is excellent, and we derive an uncertainty (1σ level) of the $|F|$'s of the order of 2%–4%. As an example, the symbols in Figs. 2(a) and 2(b) represent experimental structure factor amplitudes ($|F|$) along two high-index CTRs, where squares correspond the ''clean'' O/Fe(001)-$p(1 \times 1)$ sample, and the circles represent the data after depositing 0.5 ML of Fe on O/Fe(001)-$p(1 \times 1)$. Owing to the high $p4mm$ plane group symmetry of the structure and the occupation of in-plane positions $(x, y) = (0, 0)$ or (½, ½), the CTRs shown are representative for all data where two types of CTRs can be distinguished according to the conditions (i) $h + k = 2n + 1$ [Fig. 2(a)] and (ii) $h + k = 2n$ [Fig. 2(b)] with n integer. CTRs of each type have the same overall shape due to the identical in-plane phase factor $\exp[i2\pi(hx + ky)]$.

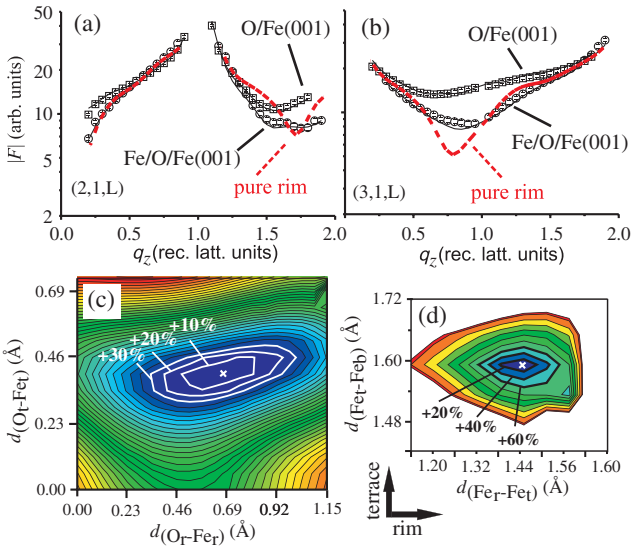

FIG. 2 (color). (a), (b): Experimental (symbols) and calculated (lines) structure factor amplitudes along two CTRs for O/Fe(001)-$p(1 \times 1)$ (squares) and 0.5 ML Fe on O/Fe(001)-$p(1 \times 1)$ (circles). The dashed red line corresponds to the calculated $|F|$'s assuming a hypothetical pure island-rim structure. (c), (d): Contour plots of GOF versus oxygen adsorption heights and first Fe-Fe interlayer spacings at the rim and terrace structures. Labels refer to Fig. 3(a). The cross marks the minimum. The contour level spacing relative to the minimum (GOF = 1.2) is indicated.

The solid lines in Fig. 2 represent the calculated $|F|$ using the program Prometheus [20]. The fit quality which is quantified by the unweighted residual (R_u) or by the goodness of fit (GOF) parameter [21] is excellent in all cases; values in the range of $R_u = 4\%$–5% were achieved corresponding to the experimental uncertainty (GOF ≈ 1). At first, it can be seen that dosing of Fe on the O/Fe(001)-$p(1 \times 1)$ surface strongly modifies the CTRs, leading to a reduction of $|F|$'s due to the antiphase scattering most pronounced in the vicinity of the antiphase condition. For the flat oxygen covered Fe(001) surface, we reproduce the results of Parihar *et al.* [16].

For the Fe-dosed sample, the CTRs were fitted by a coherent average over two structures, namely, the flat terrace structure shown on the left of Fig. 3(a) and the rim-island structure shown on the right. Large (gray) and small (red) balls represent Fe and oxygen atoms, respectively. The atoms in Fig. 3(a) are labeled accordingly by subscripts t and r for the terrace and rim (island) structure, respectively. Figure 3(b) shows the STM image ($U = -0.6$ V, $I = 100$ pA) of a sample, which is covered by ≈ 0.6 ML Fe, indicating that the SXRD analysis probes the small island case characterized by the "rim state" only. There is no terracelike structure observable; instead, bright spots within the islands are observed, which might be attributed to the somewhat different tunneling conditions. Nevertheless, the line profile in Fig. 3(c) indicates an apparent island height of nearly 2 Å, in close correspondence to the height of the small island in Fig. 3.

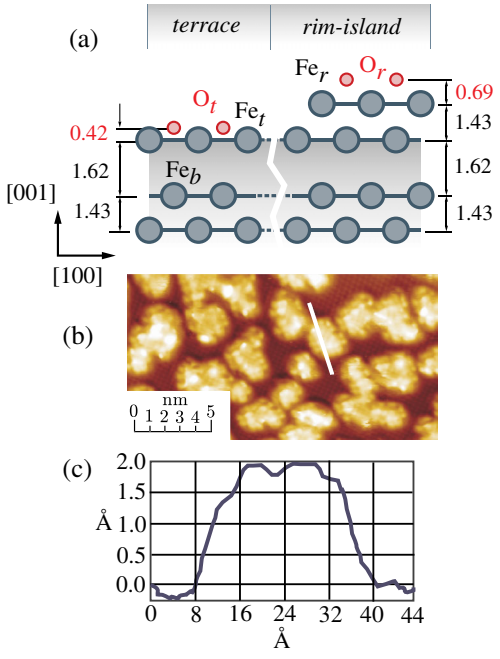

FIG. 3 (color online). (a) Model for 0.5 ML of Fe on O/Fe(001)-$p(1 \times 1)$ showing the terrace (left) and the island (right) structure. Numbers represent distances in angstrom units. Interatomic distances: O_r-Fe_t, 2.12 Å; O_r-Fe_r, 2.14 Å; O_t-Fe_b, 2.04 Å; O_t-Fe_t, 2.07 Å. (b) A 20×10 nm^2 STM image of 0.6 ML Fe/O/Fe(001)-$p(1 \times 1)$ showing the approximate morphology of the sample studied by SXRD. (c) Profile along the line in (b).

The O/Fe(001)-$p(1 \times 1)$ structure on the terrace is characterized by oxygen atoms (O_t) located 0.42 ± 0.10 Å above the level of Fe atoms labeled by Fe_t. In parallel, the first Fe-Fe interlayer spacing between Fe_t and unrelaxed Fe bulklike atoms (Fe_b) equals 1.62 ± 0.02 Å. These values are close to those found for a flat well-ordered O/Fe(001)-$p(1 \times 1)$ structure (0.48 ± 0.08 and 1.66 ± 0.02 Å according to Ref. [16]). In the island structure, the island atoms labeled Fe_r reside 1.43 ± 0.03 Å above Fe_t. Oxygen atoms O_r are located 0.69 ± 0.10 Å above Fe_r in hollow sites. Within the error bars, the spacing between Fe_t and Fe_b beneath the islands is identical to that within the terrace region (1.62 Å), indicating relaxations in the Fe_t layer below the island.

The SXRD analysis provides evidence for substantial modifications of the O/Fe(001)-$p(1 \times 1)$ structure. In combination with the STM images, we conclude that the "rim state" observed in STM images as a bright contrast (Fig. 1) is primarily related to the adsorption geometry of the oxygen and Fe island atoms, since the height difference between the terrace and the island in the 2 Å range approximately corresponds to the SXRD-derived height difference of 2.1 Å between the level of Fe_t and O_r (note that the corrugation induced by the O_t atoms is in the 0.1 Å range only [17]).

We emphasize that due to the very large and accurate CTR data, the SXRD structure model is highly precise and reliable. Many other structure models were considered, but no agreement factors even close to those achieved ($R_u \approx 4.5\%$, GOF ≈ 1) were obtained. For instance, the red dashed lines in Figs. 2(a) and 2(b) represent the calculated $|F|$'s assuming a full layer of the rim state only which significantly deviates from the experimental ones ($R_u \approx 10.3\%$, GOF $= 2.4$). In more detail, Figs. 2(c) and 2(d) show contour plots of the GOF versus the two oxygen adsorption height positions and the corresponding Fe-Fe interlayer spacings [see Fig. 3(a)]. The relative increase of GOF (in percent) from the minimum (marked by the cross) is indicated. In both cases, a clear absolute minimum is obtained.

The experimental results are supported by *ab initio* calculations, which were carried out in the framework of density functional theory (DFT) as implemented in the VASP code [22]. The exchange and correlation energies are approximated with the gradient-corrected functional of the electronic spin densities as parametrized by Perdew *et al.* [23]. The sampling of k space is performed with the Monkhorst and Pack method [24]. Projector augmented wave potentials [25], a plane-wave energy cutoff of 400 eV, and a Gaussian smearing with a width of 0.02 eV for partial occupancies are used in the calculations.

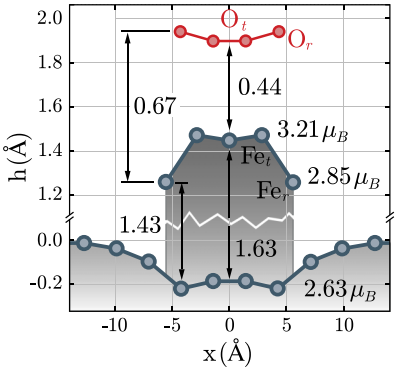

FIG. 4 (color online). Calculated geometry of an Fe nanoisland consisting of a terrace structure in the center (t) and the rim (r) structure similar to that shown in Fig. 1(a). Calculated magnetic moments for atoms Fe_t and Fe_r are indicated. Note the largely different length scales along the x and h direction.

The structure of the Fe nanoisland is approximated by a 1 nm wide stripe along the bulk [100] direction as shown in Fig. 4. Note that in order to simulate a model close to the experimental conditions, we have applied periodic boundary conditions; i.e., there is an array of islands, each being 30 Å apart from each other. The model in Fig. 4 approximately corresponds to the case shown in Fig. 1(a) characterized by a terracelike structure with atoms O_t and Fe_t in the island center and the rim structure with atoms O_r and Fe_r. This allows us to elucidate all important details of both the terrace and the island structure in one figure. The simulation of the terrace structure based on a large-ordered O/Fe(001)-$p(1 \times 1)$ structure does not lead to different results.

All positions were allowed to fully relax. Calculation of the oxygen adsorption site geometry in the center of the island (O_t) corresponding to the terrace structure, reveals close agreement with the experiment, namely, a 0.44 Å adsorption height of O_t above the level of Fe atoms (Fe_t) and an expansion of the first Fe-Fe interlayer spacing to ≈ 1.63 Å. We conclude that the structure within the center of the large island is close to that of a flat O/Fe(001)-$p(1 \times 1)$ terrace. This is also supported by the STM image shown in Fig. 1(a) in which the O/Fe(001)-$p(1 \times 1)$ structure is clearly observable inside the island.

The structure at the island rim is distinctly different from that of the terrace: The oxygen adsorption height is calculated to 0.67 Å (0.69 Å in the experiment) if the height is referenced to the Fe_r atom of the island while the first Fe-Fe interlayer distance equals 1.42 Å (1.43 Å in the experiment). The experiment and theory are in fair agreement, but we note that there is some discrepancy with regard to the width of the rim structure. In the STM image, it is about 0.5 to 1 nm in width, while it is only one atomic row (≈ 2.9 Å) in the calculations. Correspondingly, the small island ($\oslash \approx 1.5$ nm) in Fig. 1(b) entirely exhibits the rim structure, but the calculation of a relaxed island of the same size as shown in Fig. 4 already shows a terracelike structure in the interior.

Nevertheless, we can conclude that although the DFT calculations cannot provide all the details of the real structure, the most important characteristics, such as the inward relaxation of the Fe atoms and the concomitant expansion of the oxygen adsorption height, are in fair agreement with the experiment.

On the basis of the results, a straightforward answer to the longstanding problem to interpret the oscillatory behavior of the surface magnetic moment measured by SHG [14] and SPMDS [11] upon deposition of Fe can be given. At full coverage corresponding to the formation of the O/Fe(001)-$p(1 \times 1)$ surface, the magnetic moment (m) is enhanced as a consequence of the enhanced first layer spacing inducing a narrowing of the d states [10,13]. We calculate $m = 3.21\mu_B$ ($3.27\mu_B$ in Ref. [13]) and $0.22\mu_B$ for the surface Fe and the oxygen atom on the terrace, respectively. For Fe_r, the magnetic moment is reduced to $m = 2.85\mu_B$ due to the reduced interlayer spacing (1.43 Å). The oxygen magnetic moments as well as those of deeper lying Fe atoms ($\approx 2.63\mu_B$) are almost constant along the x coordinate.

A rough estimate shows that the calculated relative change of the surface Fe magnetic moment is in fair agreement with the relative magnitude of the magnetic signal oscillations (10%) reported in Ref. [14]. At half-layer coverage, 50% of the surface Fe atoms [islands, Fig. 1(b)] have a magnetic moment of $m = 2.85\mu_B$, while the other half on the terrace still has $m = 3.21\mu_B$. On average, this corresponds to a reduction of $\approx 6\%$, i.e., in the correct range, allowing us to conclude that the changes of the local atomic geometry induces the oscillating surface magnetic moments observed previously.

Finally, we note that in addition to SHG and SPMDS, which probe the average surface magnetic moment, spin polarized STM and STS experiments with atomic resolution allow us to study the local spin polarization as shown by Tange *et al.* [17] for the O/Fe(001)-$p(1 \times 1)$ terrace structure. In general, spin polarized STM and STS experiments provide the $\partial I/\partial V$ asymmetry of the tunneling current which is proportional to the spin polarization [26]. Our DFT calculations suggest that the differences between the local spin polarization of the island and terrace Fe atoms should be large enough to be detected at least in an energy range 0.2 eV away from the Fermi level. Nevertheless, a direct evaluation of the local magnetic moments is not possible.

In summary, we have presented a combined experimental and theoretical analysis of the geometric structure of oxygen atoms adsorbed on Fe nanoislands on Fe(001). STM in combination with precise SXRD experiments supported by DFT calculations have given clear evidence for mesoscopic misfit-induced modifications of the O/Fe(001) adsorption geometry including the vertical

oxygen adsorption position and the first Fe-Fe interlayer spacing, the latter sensitively affecting the magnetic moments of the Fe atoms. Our results for the O/Fe(001) adsorbate system are of importance for adsorption systems at the nanoscale in general.

We (W. F., H. L. M., K. M., and N. J.) thank the staff of the European Synchrotron Radiation Facility for their hospitality during our stay in Grenoble. We thank F. Weiss for technical support. This work is supported by the DFG through TPA5 of Grant No. SFB 762/2 2012.

*hmeyerhm@mpi-halle.de

[1] L. Pauling, J. Am. Chem. Soc. **69**, 542 (1947).
[2] R. Smoluchowski, Phys. Rev. **60**, 661 (1941).
[3] W. J. Huang, R. Sun, J. Tao, L. D. Menard, R. G. Nuzzo, and J. M. Zuo, Nat. Mater. **7**, 308 (2008).
[4] O. Mironets, H. L. Meyerheim, C. Tusche, V. S. Stepanyuk, E. Soyka, P. Zschack, H. Hong, N. Jeutter, R. Felici, and J. Kirschner, Phys. Rev. Lett. **100**, 096103 (2008).
[5] H. L. Meyerheim, E. D. Crozier, R. A. Gordon, Q. F. Xiao, K. Mohseni, N. N. Negulyaev, V. S. Stepanyuk, and J. Kirschner, Phys. Rev. B **85**, 125405 (2012).
[6] V. S. Stepanyuk, D. I. Bazhanov, A. N. Baranov, W. Hergert, P. H. Dederichs, and J. Kirschner, Phys. Rev. B **62**, 15 398 (2000).
[7] M. V. Rastei, B. Heinrich, L. Limot, P. A. Ignatiev, V. S. Stepanyuk, P. Bruno, and J. P. Bucher, Phys. Rev. Lett. **99**, 246102 (2007).
[8] J. Chen, M. Drakaki, and J. L. Erskine, Phys. Rev. B **45**, 3636 (1992).
[9] K. O. Legg, F. Jona, D. W. Jepsen, and P. M. Marcus, Phys. Rev. B **16**, 5271 (1977).
[10] S. R. Chubb and W. E. Pickett, Phys. Rev. Lett. **58**, 1248 (1987).
[11] F. Bisio, R. Moroni, M. Canepa, L. Mattera, R. Bertacco, and F. Ciccacci, Phys. Rev. Lett. **83**, 4868 (1999).
[12] R. Bertacco and F. Ciccacci, Phys. Rev. B **59**, 4207 (1999).
[13] P. Blonski, A. Kiejna, and J. Hafner, Surf. Sci. **590**, 88 (2005).
[14] M. Nyvlt, F. Bisio, J. Franta, C. L. Gao, H. Petek, and J. Kirschner, Phys. Rev. Lett. **95**, 127201 (2005).
[15] F. Donati, P. Sessi, S. Achuilli *et al.*, Phys. Rev. B **79**, 195430 (2009).
[16] S. S. Parihar, H. L. Meyerheim, K. Mohseni, S. Ostanin, A. Ernst, N. Jedrecy, R. Felici, and J. Kirschner, Phys. Rev. B **81**, 075428 (2010).
[17] A. Tange, C. L. Gao, B. Y. Yavorsky, I. V. Maznichenko, C. Etz, A. Ernst, W. Hergert, I. Mertig, W. Wulfhekel, and J. Kirschner, Phys. Rev. B **81**, 195410 (2010).
[18] J. Kirschner, Surf. Sci. **138**, 191 (1984).
[19] C. M. Schleptüz, R. Herger, P. R. Willmott, B. D. Patterson, O. Bunk, Ch. Brönnimann, B. Henrich, G. Hülsen, and E. F. Eikenberry, Acta Crystallogr. Sect. A **61**, 418 (2005).
[20] U. H. Zucker, E. Perenthaler, W. F. Kuhs, R. Bachmann, and H. Schulz, J. Appl. Crystallogr. **16**, 358 (1983).
[21] The unweighted residual (R_u) is defined as $R_{\mathrm{u}} = \sum ||F^{\mathrm{obs}}| - |F^{\mathrm{calc}}|| / \sum |F^{\mathrm{obs}}|$. GOF is defined by $\mathrm{GOF} = \sqrt{[1/(N-P)]\sum[(|F^{\mathrm{obs}}| - |F^{\mathrm{calc}}|)^2/\sigma^2]}$. Here, F^{obs}, F^{calc} are the experimental and calculated structure factors, respectively, while N and P represent the number of data points and the number of refined parameters. The standard deviation of F_{obs} is given by σ. The summation runs over all data points.
[22] G. Kresse and J. Hafner, Phys. Rev. B **47**, 558 (1993).
[23] J. P. Perdew, K. Burke, and M. Ernzerhof, Phys. Rev. Lett. **77**, 3865 (1996).
[24] H. Monkhorst and J. Pack, Phys. Rev. B **13**, 5188 (1976).
[25] P. E. Blochl, Phys. Rev. B **50**, 17 953 (1994).
[26] H. Oka, P. A. Ignatiev, S. Wedekind, G. Rodary, L. Niebergall, V. S. Stepanyuk, D. Sander, and J. Kirschner, Science **327**, 843 (2010).